

## CHANNEL CONVECTION AND FORMATION OF FRECKLES

S.D. Felicelli

Grupo de Mecánica Computacional  
Centro Atómico Bariloche, 8400 Bariloche, Argentina

P.K Sung and D.R. Poirier

Dept. Materials Science and Engineering  
University of Arizona, Tucson, AZ 85721, U.S.A.

### ABSTRACT

In this paper, the initiation of a channel was investigated with two-dimensional simulations of the solidification of a Ni-base superalloy. It was observed that channels started at the top of the mushy zone, became somewhat deeper for a short period while the front advanced, and then stayed "behind" as the front continued upward. This process was helped by remelting; *i.e.*, the channel partially melted downward from the front and deeper into the mushy zone.

### INTRODUCTION AND DESCRIPTION

A severe form of macrosegregation, known as "freckles," is cause to scrap directionally solidified (DS) and dendritic single-crystal (SC) castings of Ni-base superalloys, which are used as critical components in gas-turbine engines. Freckles are observed as long and narrow trails, aligned roughly parallel to the direction of gravity in both DS- and SC-castings and are enriched in the normally segregating elements and depleted in the inversely segregating elements.<sup>[1]</sup> The ability to predict the formation of freckles in the castings is a critical issue at the present time. In this paper, the initiation of a channel is investigated with two-dimensional simulations of the solidification of a Ni-base superalloy.

The transport phenomena during directional solidification of multicomponent alloys are modeled by a mathematical formulation, which comprises the continuity equation, the energy equation, the momentum equation, and the solute conservation equations for all alloy elements. A comprehensive description of the model and the finite element methodology are given by Felicelli *et al.*<sup>[2,3]</sup> and not repeated here.

As a test alloy, the commercial alloy René N5 is selected; it is one of the second-generation SC-superalloys that show excellent creep-resistance at high temperatures. The composition of the simulated alloy is Ni-6.41Ta-7.11Cr-6.25Al-7.35Co-4.92W- 2.89Re-1.42Mo, all in wt pct. The model requires an extensive list of transport properties and thermodynamic properties, which are given in Reference 4, and not repeated here.

The alloy is directionally solidified by simulation in a rectangular mold of 10 mm in width and 50 mm in height; gravity acts downward. Initially, the mold is filled with an all-liquid alloy of the nominal composition in a stable vertical temperature gradient such that the bottom temperature is slightly above that of the liquidus temperature. A constant thermal gradient ( $G = 4000 \text{ K m}^{-1}$ ) is imposed at the top, and a constant cooling rate ( $r = 0.22 \text{ K s}^{-1}$ ) is applied at the bottom. Lateral walls are thermally insulated. Initially small random perturbations are introduced in each solute concentration field in order to excite the convection. A no-slip condition is used for velocity at all casting surfaces. Based on a detailed analysis of solidification conditions for this alloy,<sup>[4]</sup> it was known that these thermal boundary conditions would result in a freckling-case.

In this investigation, the domain was discretized with a uniform mesh of 40 elements in the horizontal direction and 500 elements in the vertical direction. The elements were only  $0.25 \text{ mm} \times 0.1 \text{ mm}$  (about  $0.7 d_1$  by  $0.6 D/V$ , where  $d_1$  is the primary dendrite arm spacing,  $D$  is the diffusion coefficient

of the solute in the liquid, and  $V$  is the growth rate). These are even smaller than our most stringent recommendation<sup>[4]</sup> that the element be no larger than  $2 d_1$  in the horizontal direction and  $1.5 D/V$  in the vertical direction.

## RESULTS

Figure 1 is a plot of density of the liquid *versus* distance through part of the mushy zone and the overlying liquid on the centerline of the casting at 250 s of solidification. At this time, there is no channel. Most of the liquid in the overlying liquid has a stabilizing density gradient because of the positive thermal gradient. However, just above the position of the dendrite tips, there is a layer of small thickness, which has an unstable density gradient because of the solute redistribution during solidification. The thickness of this layer is slightly greater than  $D/V$ . Figures 2a and 2b show the thermosolutal convection and density of liquid at 300 s, which is about 25 s before a channel initiates. In Figure 2a, the strongest upward flow occurs at  $x = 0.007$  m ( $x$  measured from the left side) where the channel eventually initiates. Notice too that the convection cells only penetrate the mushy zone to where the fraction of liquid is about 0.95 or greater. As shown in Figure 2b, there is a higher-density layer with unstable density gradient just above the dendrite tips (dotted line), and the unstable layer induces the well-organized convection cells with a width of approximately 1.5 mm (Figure 2a). Associated with the strongest pair of convection cells, the isodensity contours have developed small amplitudes, which of course contribute to the convective instability of the liquid.

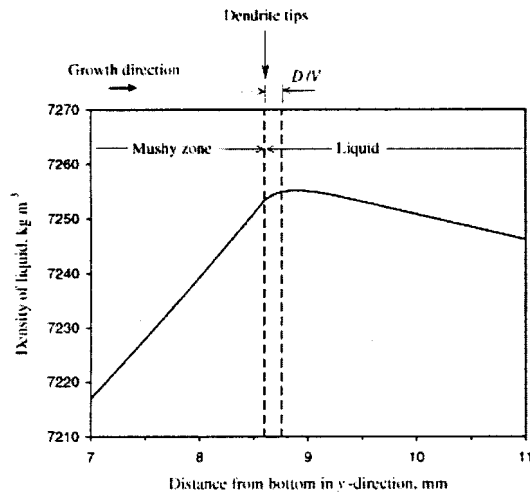


Fig. 1 - Density of liquid *versus* distance through part of mushy zone and overlying liquid on centerline of casting at 250 s of solidification with  $G = 4000 \text{ K m}^{-1}$ ,  $c = 0.22 \text{ K s}^{-1}$ .

Figure 3 shows the growth rate and the maximum velocity of the upward liquid flow at the location of channel formation. At 315 s the contours of constant fraction liquid near the dendrite tips deflect downward under the rising liquid at  $x = 0.007$  m. The growth rate, measured on both sides of this small depression, increases to about  $0.04 \text{ m s}^{-1}$  at 318 s and then develops the squiggly pattern. For times between 315 s and 325 s, the small depression centered at  $x = 0.007$  m came and went. Finally at 325 s the depression developed into the beginning of a channel, when the maximum velocity of the liquid increased rapidly and exceeded the growth rate.

The channel at 340 s is shown as Figure 4. The well-organized convection cells, which existed at 300 s as shown in Figure 2a, are now agglomerated into bigger cells with a width of approximately 3 mm

(Figure 4a). As the growth front advances, the channel within the mushy zone elongates and becomes a freckle in the completely solidified casting.

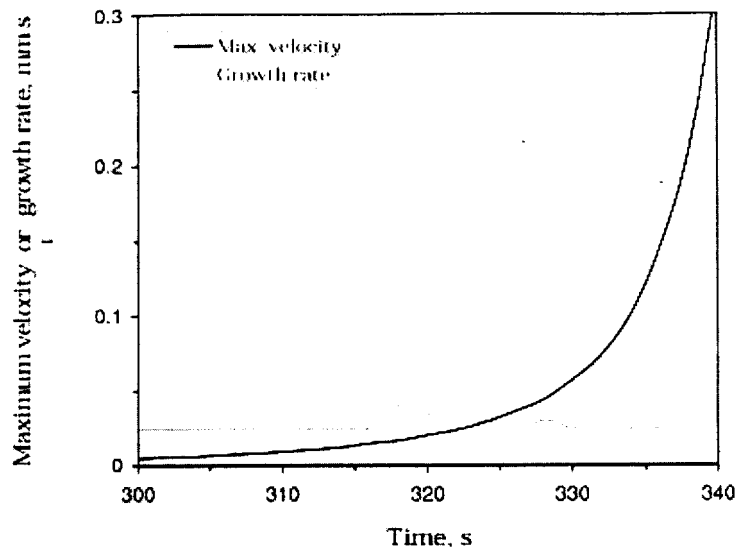


Fig. 3 - Relation between growth rate and maximum velocity of upward liquid flow at the location of channel formation.

Prior to when the channel initiated at 325 s, the fraction liquid contour of unity depressed slightly at  $x = 0.007$  m. This is unlike the upswing preceding channel nucleation as modeled by Schulze and Worster.<sup>[5]</sup> They also predicted that the fledgling channels emerge from liquid inclusions in the interior of the mushy zone. We observed that the channel starts at the top of the mushy zone, became somewhat deeper for a short period (approximately 15 s) while the front advanced, and then stayed "behind" as the front continued upward. This process is helped by remelting; *i.e.*, the channel partially melts downward from the front and deeper into the mushy zone. Remelting occurs because the upward flowing liquid in the channel has a lower freezing temperature, largely because it is depleted in Re and W. Schulze and Worster<sup>[5]</sup> invoked several assumptions not used by us which could account for the qualitative differences in how a channel nucleates. Perhaps the most important difference is that they assumed that the nondimensional permeability ( $\Pi$ ) was given by

$$\Pi = \phi^3 \quad [1]$$

where  $\phi$  is the volume fraction of liquid. The permeability function that we use is based on calculations of flow through dendritic microstructures and can be found in References 2 and 3. At 0.95 fraction liquid the nondimensional permeability used by Schulze and Worster<sup>[5]</sup> is about seven times greater than our calculated permeability for flow parallel to the primary dendrite arms. The ratio is greater for flow perpendicular to the primary dendrite arms. At a fraction liquid of 0.8, the ratio is about 13. Hence, it appears that the strength of the convection in the high fraction liquid part of the mushy zone is overestimated by Eq. [1] and could account for nucleation of a liquid inclusion in the interior of the mushy zone. Other assumptions, which we do not invoke, are Stokes flow in the liquid region; infinite Prandtl and Lewis numbers; neglect of thermal buoyancy (probably not critical); and local thermodynamic equilibrium in the mushy layer (also not important in present context). Finally, the parameters used by Schulze and Worster<sup>[5]</sup> are characteristic of experiments using ammonium-

chloride solutions, which of course are very different in metallic alloys.

As a measure of the strength of interdendritic convection in mushy zone, a Rayleigh number was devised by Worster.<sup>[6]</sup> For multicomponent alloys, the mushy-zone Rayleigh number ( $Ra_m$ ) is extended as:

$$Ra_m = \frac{\Delta\rho g \Pi_o L}{\mu \kappa} \quad [2]$$

where  $\mu$  is the viscosity,  $\kappa$  is the thermal diffusivity,  $g$  is the gravity acceleration,  $\Pi_o$  is the characteristic permeability,  $L$  is thermal length scale (thickness of mushy zone), and  $\Delta\rho$  is the density difference in mushy zone defined as:

$$\Delta\rho = \rho_o \left[ \beta_T (T_E - T_o) + \sum_{j=1}^N \beta_C^j (C_E^j - C_o^j) \right] \quad [3]$$

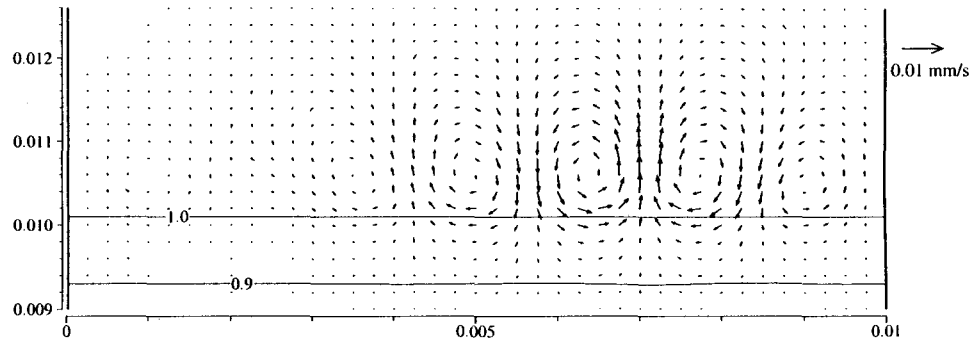
where  $\beta_T$  is the thermal expansion coefficient;  $\beta_C^j$  is the solutal expansion coefficient of element  $j$ ;  $N$  is the number of elements in the alloy;  $T_E$  is the eutectic temperature;  $T_o$  is the liquidus temperatures;  $C_E^j$  is the eutectic composition;  $C_o^j$  is the initial composition; and  $\rho_o$  is the reference density of the alloy at  $T_o$  and  $C_o^j$ .

Bergman *et al.*<sup>[7]</sup> assumed that  $\Pi_o = d^2$ , where  $d$  is the primary dendrite arm spacing, and found that the critical Rayleigh number dividing cases of no channels and cases with channels is in the range of 35 to 50. Our calculated value is about 25. Bergman *et al.*<sup>[7]</sup> studied hypoeutectic Pb-Sn alloys that were directionally solidified, but the thermal gradients were only between 4 and 8 K cm<sup>-1</sup>. Since the instability is associated with the layer of thickness  $D/V$  just above the dendrite tips, it is probably fortuitous that our critical value of 25 is reasonably close to the range found by Bergman *et al.*<sup>[7]</sup> with a Rayleigh number based on the characteristics of the mushy zone. Notice too that most of the overlying liquid provides a stabilizing density variation (Figure 1) so it is reasonable to hypothesize that there is a competition between the unstable layer and the stabilizing overlying liquid; future attempts to identify critical conditions should take this into account.

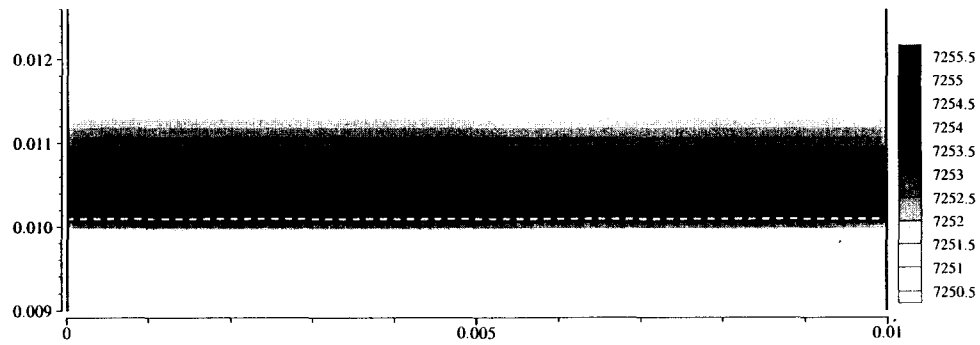
This work was supported by the Division of International Programs of the National Science Foundation (U.S.A.) and by Consejo Nacional de Investigaciones Científicas y Técnicas (Argentina), under the frame of the international cooperation project "Simulation of Defects in Castings." Also, P.K.S. and D.R.P. appreciate the grant provided by National Science Foundation (DMR-9901290), and S.D.F. appreciates the grant provided by Agencia Nacional de Promoción Científica y Tecnológica (PICT98 12-03239). Our many discussions with Professor J.C. Heinrich of The University of Arizona on subjects of transport phenomena and finite element formulations have always been very helpful.

#### REFERENCES

1. A.F. Giamei and B.H. Kear: *Metall. Trans.*, 1970, vol. 1, pp. 2185-92.
2. S.D. Felicelli, D.R. Poirier, and J.C. Heinrich: *J. Cryst. Growth*, 1997, vol. 177, pp. 145-61.
3. S.D. Felicelli, J.C. Heinrich, and D.R. Poirier: *Inter. J. Numer. Meth. Fluids.*, 1998, vol. 27, pp. 207-27.
4. P.K. Sung, D.R. Poirier, and S.D. Felicelli: *Inter. J. Numer. Meth. Fluids*, accepted for publication, 2000.
5. T.P. Schulze and M.G. Worster: *J. Fluid Mech.*, 1999, vol. 388, pp. 197-215.
6. M.G. Worster: *J. Fluid Mech.*, 1992, vol. 237, pp. 649-69.
7. M.I. Bergman, D.R. Fearn, J. Bloxham, and M.C. Shannon: *Metall. Mater. Trans. A.*, 1997, vol. 28A, pp. 859-66.



(a)



(b)

Fig. 2 – Thermosolutal convection at 300 s: (a) velocity vectors and contour lines of fraction liquid; (b) density of liquid in  $\text{kg m}^{-3}$ , dashed line shows dendrite tips. Dimensions are in m.

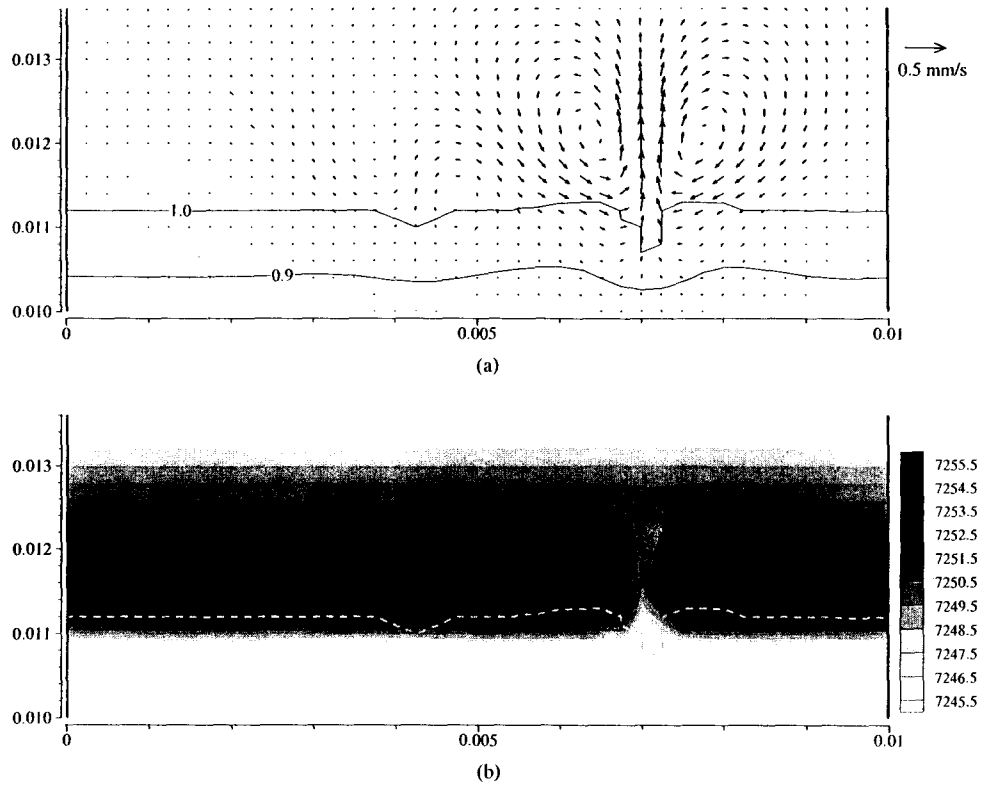


Fig. 4 – Thermosolutal convection at 340 s: (a) velocity vectors and contour lines of fraction liquid; (b) density of liquid in  $\text{kg m}^{-3}$ , dashed line shows dendrite tips. Dimensions are in m.